Optical characterization of $LiNbO_3 : Yb^{3+}$ crystals

1999 J. Phys.: Condens. Matter 11 311

(http://iopscience.iop.org/0953-8984/11/1/026)

J. Phys.: Condens. Matter **11** (1999) 311–320. Printed in the UK PII: S0953-8984(99)93327-1

Optical characterization of $LiNbO_3$:Yb^{3+} crystals

E Montoya†, A Lorenzo and L E Bausá

Departamento de Física de Materiales, Universidad Autónoma de Madrid, Cantoblanco, 28049-Madrid, Spain

Received 16 April 1998, in final form 12 October 1998

Abstract. A spectroscopic study of Yb^{3+} ions in $LiNbO_3$ and $LiNbO_3$:MgO monocrystals is presented. Polarized absorption and luminescence spectra at low and room temperature allow the identification of the energy levels of the Yb^{3+} ion in these matrices. The fluorescence decay time has also been investigated and shows an exponential behaviour with a lifetime value of 530 μs at 15 K for Yb^{3+} singly doped $LiNbO_3$.

Site selective spectroscopy measurements detect the existence of non-equivalent positions of the Yb^{3+} which can be related to the presence of Yb^{3+} in the Li^+ octahedral site but with slightly different shifts from the regular Li site. Codoping with MgO induces new absorption and emission bands as a consequence of new Yb^{3+} centres which appear in the matrix due to the presence of Mg^{2+} ions.

1. Introduction

Since the first growth of $LiNbO_3$ in the sixties, an increasing interest has been paid to determining the promising features of this material. Its excellent non-linear properties have made $LiNbO_3$ one of the best candidates for electro-optic devices, as well as for storage of information and holography. It can be easily doped with rare earth (RE) ions to develop minilasers with self-frequency doubling, self-Q-switching and self-mode-locking [1].

In this sense, the trivalent Yb ion has attracted attention as a dopant in laser materials. Its optical properties have been studied in a variety of systems and laser action has been obtained in different hosts [2–6]. The Yb^{3+} electronic configuration is $4f^{13}$ and thus, only two manifold states are possible: the ground $^2F_{7/2}$ and the excited $^2F_{5/2}$ state separated by an energy of around 10 000 cm^{-1}. This energy fits quite well the emission of InGaAs diode lasers. Due to its high cross-section, the Yb^{3+} ion has been used as a sensitizer for other RE ions to increase their pumping efficiency, as in the case of Yb–Er codoped systems, via energy transfer [7]. Another favourable feature of Yb^{3+} ions is the negligible nonradiative relaxation rate and the fact that there are no mechanisms competing with the laser transition, such as excited-state absorption or up-conversion processes.

Previous studies concerning the spectroscopy of Yb^{3+} doped $LiNbO_3$ are scarce [2, 8] and a deep spectroscopic study, including low temperature measurements, becomes necessary to obtain an accurate scheme of the energy level positions and the optical behaviour of the system.

In this work, low temperature polarized absorption and emission spectra have been studied to determine the crystal field energy levels of Yb^{3+} ions in $LiNbO_3$ single crystals. In order to investigate the possible presence of spectroscopically non-equivalent active Yb^{3+} centres, as in the case of other trivalent ions, site selective experiments have been used.

† Corresponding author. E-mail address: eladio.montoya@uam.es.

0953-8984/99/010311+10$19.50

Fluorescence lifetime measurements have been also performed and an estimation of the radiative transition probability from the absorption spectra has been carried out.

From the viewpoint of lasing and device fabrication, it is important to minimize photorefractive damage in $LiNbO_3$. The addition of around 5 mol% MgO has been proved to effectively reduce this effect [9]. Thus, the influence of Mg^{2+} ions on the optical properties of the Yb^{3+} ions in the $LiNbO_3$ host has also been studied.

2. Experiment

Yb^{3+}:$LiNbO_3$ and Yb^{3+}, MgO:$LiNbO_3$ crystals were grown along the *c*-axis from the congruent melt, [Li]/[Nb] = 0.942, by the Czochralski method using grade I Johnson–Matthey Li_2O and Nb_2O_5. Yb_2O_3 and MgO were added to obtain 1 mol% of Yb^{3+} and 6 mol% of MgO in the melt. At the end of the growth an electric field parallel to the *c*-axis was applied in order to avoid the formation of ferroelectric domains.

Yb concentrations in the samples, estimated by Rutherford backscattering measurements, were 1.2 and 1.03 mol% for the case of singly doped samples and the MgO–Yb co-doped crystals, respectively. To perform the spectroscopic measurements, plates were cut and polished with the surfaces perpendicular or parallel to the *c*-axis.

The absorption spectra were taken with a Hitachi U-3501 spectrophotometer. The emission spectra were obtained by pumping with a pulsed Spectra Physics Quanta-Ray 730 MOPO or a Spectra Physics CW 3900 Ti:sapphire laser. The luminescence was detected using a germanium or a silicon photodiode detector. The light was focused on the entrance slit of a SPEX 500M monochromator. Low temperature absorption and emission spectra at 15 K (LT) were performed by using a Leybold–Heraeus closed cycle He cryostat.

3. Results and discussion

3.1. Absorption spectra

The study of the absorption spectra allows us to determine the character of the involved transitions (electric/magnetic dipolar) between the different Stark sublevels, as well as to label the crystal field energy levels for Yb^{3+} ions in $LiNbO_3$. The absorption spectra have been obtained for different polarization configurations: α configuration, which corresponds to the case of the light beam parallel to the ferroelectric *c*-axis of the sample; σ configuration, with the electric field of the light perpendicular to the *c*-axis of the sample, and π configuration, in which the electric field of the incident beam is parallel to the *c*-axis.

The character of the involved transitions between the crystal field sublevels has been determined by comparing the σ and π polarized spectra at LT. The obtained α and σ spectra were very similar and, therefore, it is possible to conclude that the involved transitions have electric dipole character.

Figure 1 shows the polarized absorption (σ and π) spectra of Yb^{3+}:$LiNbO_3$ at two different temperatures. The spectra corresponding to the α configuration are not included since they are practically indistinguishable from the σ polarized spectra.

In $LiNbO_3$ crystals RE^{3+} ions usually enter Li^+ lattice sites and the local symmetry is C_3 [10]. For the case of Yb^{3+} ions in this crystal, it is expected that this C_3 symmetry splits the two, $^2F_{7/2}$ and $^2F_{5/2}$, free ion energy states into four and three doubly degenerate crystal field levels respectively, their character being E_1 or E_2, as follows from group theory. As a matter of fact, the spectra shown in figure 1 can be well analysed on the basis that the local symmetry at the Yb^{3+} site is C_3.

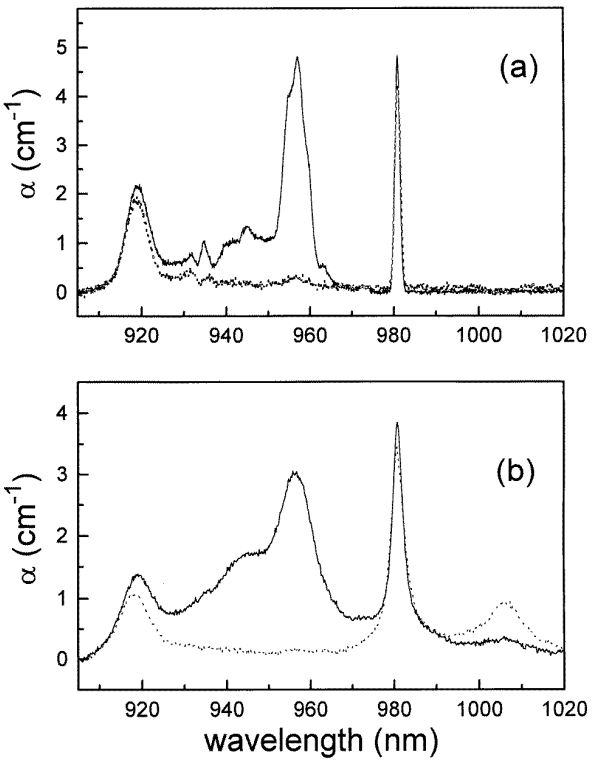

Figure 1. Polarized absorption spectra of Yb^{3+} doped $LiNbO_3$: (a) low temperature and (b) room temperature. Continuous line: σ configuration; dashed line: π configuration.

Three main bands centred at 918 nm, 956 nm and 980 nm are clearly detected for the LT σ polarized spectrum. Since at low temperature the most populated Stark level is the lowest energy level of the $^2F_{7/2}$ ground state, these bands can be associated with the transitions from this energy level to the three Stark levels of the excited state, $^2F_{7/2}(1) \rightarrow {}^2F_{5/2}$ (3), (2) and (1) respectively. Therefore, it is possible to locate the Stark energy levels of the $^2F_{5/2}$ excited multiplet. Additionally, by comparing the LT σ and π spectra, the character of the Stark sub-levels of the excited and fundamental states can be obtained by using the electric dipole selection rules: $E_2 \rightarrow E_2$ type transitions are allowed in π, σ and α configurations, $E_1 \rightarrow E_1$ type transitions are allowed only in the π configuration and $E_{2(1)} \rightarrow E_{1(2)}$ are σ and α allowed.

A main feature is observed when comparing the σ and π spectra: the central band appearing at 956 nm in the σ spectrum is not detected in the π one. However, the remaining bands are observed for both configurations. This indicates that the character of the fundamental Stark level of the ground state is E_2 and the three sublevels of the excited group show an E_2, E_1 and E_2 character in order of increasing energy. Figure 2 shows the energy position and the character of the different Stark levels of the $^2F_{5/2}$ excited state.

A more detailed inspection of the LT absorption spectra reveals a certain substructure. In the 930–940 nm region several weak peaks are observed and a triplet structure is also appearing around the band peaking at 957, which is associated with a single Stark transition. This structure can be related to strongly phonon-coupled transitions involving components of the split $^2F_{5/2}$ excited state. In fact, previous studies pointed out the strong electron–phonon interaction in Yb^{3+} doped systems [11, 12].

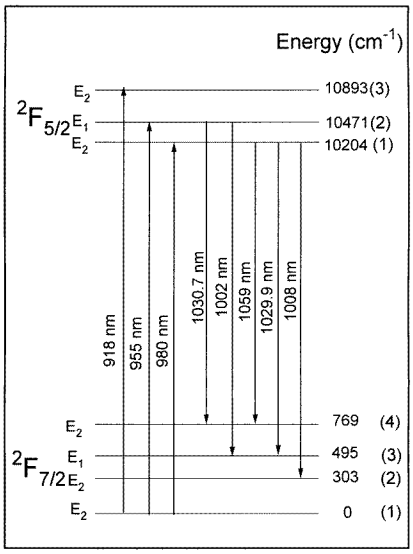

Figure 2. Crystalline field energy level scheme of Yb^{3+} ion in $LiNbO_3$.

As shown in figure 1(b), at room temperature all the bands become broader and a big hump appears, hiding the aforementioned vibronic structure. In fact, the broad bands in the region 900–965 nm correspond to strongly phonon-coupled transitions to higher components of the split $^2F_{5/2}$ state. However, an important feature concerning the characterization of the Stark transitions is the presence of a new band at 1008 nm in π polarization when the temperature is increased. This 'hot' band corresponds to the absorption from the first excited Stark level of the fundamental $^2F_{7/2}$ state to the lowest energy level of the $^2F_{5/2}$ excited state. This shows that thermal effects play an important role in the population of the Stark sublevels. A detailed study of the thermal effects and the evolution of the optical spectra with temperature has recently been reported for this system [13]. According to the selection rules, the first excited level of the fundamental group $^2F_{7/2}(2)$ can be labelled as E_2.

3.1.1. Codoping with MgO. Figure 3(a) and (b) shows the polarized absorption spectra (π and σ) at two different temperatures for a Yb^{3+},MgO:$LiNbO_3$ codoped sample. Three main features are observed when these spectra are compared with those of figure 1.

Firstly, as observed from the area of the spectra, as well as from the analysis of Yb concentration in the sample, when co-doping with MgO the segregation coefficient of Yb^{3+} slightly decreases relative to that of the singly doped samples. A decrease of around 15% in the Yb content is obtained. This effect has been already observed for other RE^{3+}:MgO codoped $LiNbO_3$. It indicates that the incorporation of RE^{3+} is affected due to the ability of Mg^{2+} ions to enter the $LiNbO_3$ lattice. However, the diminution of the RE^{3+} incorporation for most cases is more important (of the order of 50%) than that observed for Yb^{3+} ions. Thus, the lower diminution in the segregation coefficient of Yb^{3+} ions, compared to other dopant ions, could be associated with the lower ionic radius of Yb^{3+} ion, which favours its incorporation into the $LiNbO_3$ lattice.

Secondly, codoping with MgO produces a slight broadening of the absorption lines. This inhomogenous broadening, already reported for other RE^{3+},MgO codoped $LiNbO_3$, is a consequence of a greater number of defects in the host due to Mg^{2+} incorporation.

Finally, a new band (σ–π polarized) located at the high energy side of the absorption spectra is detected at 908 nm at room and LT. This observation indicates that at least one new

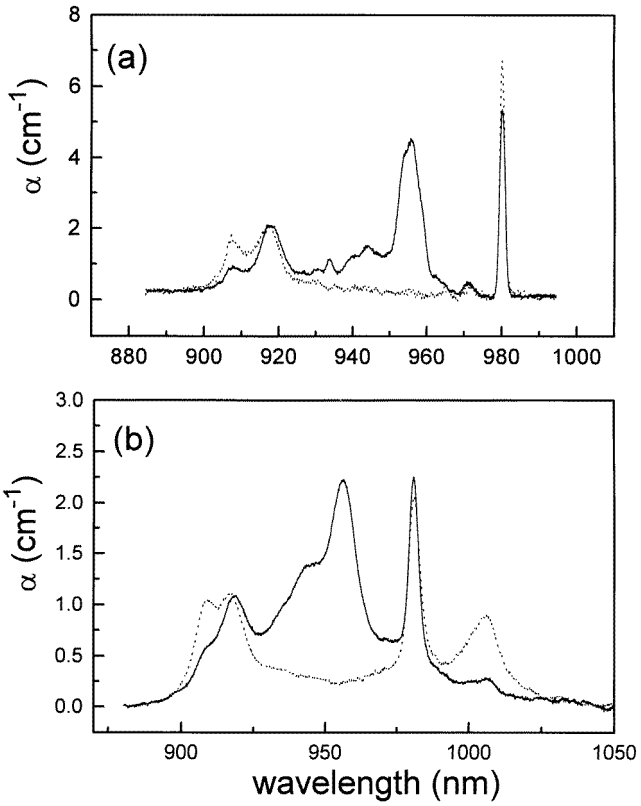

Figure 3. Polarized absorption spectra of Yb^{3+}:Mg:$LiNbO_3$: (a) low temperature and (b) room temperature. Continuous line: σ configuration; dashed line: π configuration.

Yb^{3+} centre is appearing induced by the presence of Mg^{2+} ions. This has also been reported to occur for other RE^{3+} (or transition metal ion) MgO codoped $LiNbO_3$ samples [14]. In our case, the new band appears close to the band associated with the transition $^2F_{7/2}(1) \rightarrow {}^2F_{5/2}(3)$ observed for the singly doped crystals and keeps the same polarization character.

3.2. Fluorescence spectra

In order to determine the Stark energy levels of the ground state, the emission spectra were studied. Figure 4(a) shows the polarized emission spectra at LT by exciting at the high energy absorption line (918 nm). They consist of four main bands located at 981 nm, 1006 nm, 1030 nm and 1060 nm, which can be associated with the transitions from the lowest energy level of the excited $^2F_{5/2}$ state to each of the four levels of the $^2F_{7/2}$ fundamental state. The peak at 981 nm coincides with the lower energy peak in the absorption spectra, and it is due to the transition from the lowest Stark level of the excited state, $^2F_{5/2}(1)$, to the lowest Stark level of the fundamental state, $^2F_{7/2}(1)$.

A detailed inspection of the emission spectra at LT reveals two weak peaks at 988.7 and 999.5 nm which correspond to emissions from the upper levels of the excited state to the first and second excited levels of the fundamental state. The full energy scheme, as well as the assignment of the observed transitions (absorption and emission) at LT, is shown in figure 2.

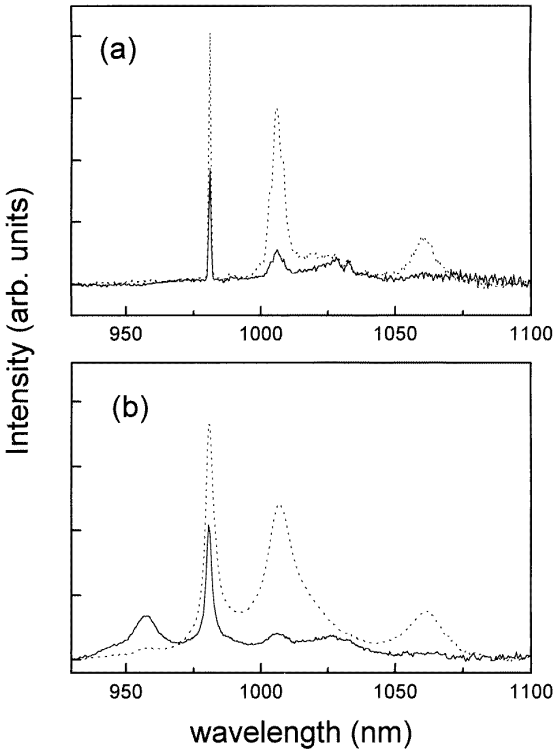

Figure 4. Emission spectra of Yb^{3+} doped $LiNbO_3$ under excitation at 918 nm. (a) Low temperature and (b) room temperature. Continuous line: σ configuration; dashed line: π configuration.

Strong changes are detected when comparing the low and room temperature emission spectra. As shown in figure 4(b), at room temperature the bands are significantly broader. The characteristic feature of these room temperature emission spectra is the narrow band at 980 nm and the phonon broadened bands in the 1–1.07 μm range.

Figure 4(b) also shows the appearance of new bands which emerge due to the effect of thermal population of the excited sub-levels of the $^2F_{5/2}$ state. The new line appearing at 955 nm can be associated with the transition from the $^2F_{5/2}(2)$ excited Stark level state to the $^2F_{7/2}(1)$ lowest energy level of the fundamental state.

At this point, it is important to note that the relative intensities of the emission lines may be different to those shown in the spectra of figure 4. According to previous studies, reabsorption phenomena of the photoluminescence are important in the case of Yb-doped materials and they influence the shape of the emission spectra. Even if the experimental conditions used in this work minimize the reabsorption, the influence of this effect is difficult to estimate. Reabsorption can be important for the line peaking at 980 nm and for transitions originated from thermally populated high-lying sublevels of $^2F_{5/2}$ state, so the actual intensity of the line peaking at 980 nm and of the energetically close-lying bands may be higher than those shown in figure 4.

Lifetime measurements were performed for the different emission bands appearing in the spectra. The fluorescence decay time showed an exponential behaviour with a lifetime value of 538 μs at 15 K. This value increases up to 630 μs at room temperature, due to the above mentioned radiation trapping effect, which has been shown to be temperature dependent [13].

Due to the small number of states in this system, the Judd–Ofelt theory cannot be applied to predict the radiative transition probability. However, for this two-state system it can be estimated from the absorption spectra.

Using Weber's expression [15] the radiative transition probability can be written as:

$$A_{if} = \frac{g_f}{g_i}\frac{8\pi n^2}{N\lambda_0^2}\int \alpha(\nu)\,\mathrm{d}\nu = \frac{g_f}{g_i}\frac{8\pi n^2}{N\lambda_0^4}\int \alpha(\lambda)\,\mathrm{d}\lambda$$

where N is the concentration of Yb^{3+} inside the crystal, n is the refractive index, λ_0 is the mean wavelength of the absorption peak (950 nm) and g_i and g_f are the degeneracies of the initial and final states, six and eight respectively. Because of the anisotropy of $LiNbO_3$ we must define the absorption probability (A) as a function of the integrated absorbance in σ and π polarization (Γ_σ and Γ_π respectively).

$$A = \frac{g_f}{g_i}\frac{8\pi n_\pi^2 c}{N\lambda_0^4}\Gamma_\pi + 2\frac{g_f}{g_i}\frac{8\pi n_\sigma^2 c}{N\lambda_0^4}\Gamma_\sigma$$

where n_σ and n_π are the refractive indexes defined as a function of the wavelength by the Sellmeier relations.

At room temperature the integrated absorbances are $\Gamma_\sigma = 116.4$ cm^{-1} nm and $\Gamma_\pi = 57.26$ cm^{-1} nm. From here, the transition probability, A, is 1860 s^{-1} and the radiative transition lifetime is $\tau_r = 537$ μs, which is in good agreement with the measured value at low temperature for which the contribution of radiation trapping is negligible. From this result it is possible to conclude that the quantum efficiency of Yb^{3+} in $LiNbO_3$ is very close to unity. Indeed, a negligible non-radiative relaxation rate is expected in this matrix since the energy between states (around 10 000 cm^{-1}) is large compared to the effective phonon energy (880 cm^{-1}) [16] and the multiphonon non-radiative de-excitation would need the participation of at least 11 effective phonons.

3.2.1. Site selective spectroscopy. In the case of Yb^{3+}-doped LiNbO crystals Rutherford backscattering/channelling measurements (RBS) [10] have unambiguously shown that Yb^{3+} ions occupy an Li^+ position although slightly shifted, around 0.3 Å, from the regular Li^+ site along the c-axis to the nearest plane of oxygen ions. However, to investigate the presence of possible multicentres, site selective fluorescence experiments have been performed.

Figure 5(a) shows two LT emission spectra for two different excitation wavelengths. The main differences between them correspond to slight shifts of the bands, in particular that one observed in the low energy emission side at 1060 nm. The corresponding excitation spectra have also been studied and a detailed part is shown in figure 5(b). There, the clearest result concerning the transition $^2F_{7/2}(1) \rightarrow {}^2F_{5/2}(3)$ is depicted. As shown, the excitation spectra peak in different positions when changing the emission wavelength. These excitation spectra are in good agreement with the corresponding $^2F_{7/2}(1) \rightarrow {}^2F_{5/2}(3)$ absorption, which clearly contains the contribution of at least two Yb^{3+} centres.

A detailed range of the selectively excited emission spectra is shown in figure 6, where the emission at around 1 μm, $^2F_{5/2}(1) \rightarrow {}^2F_{7/2}(2)$, has been shown for different excitation wavelengths. A clear structure can be resolved, indicating the presence of at least four centres whose associated relative emission intensities change with the excitation energy. According to that, several Yb^{3+} centres with slightly different energy levels are contributing to the optical spectra. Since small differences are observed among the emission lines associated with the different centres, the perturbation affecting the different Yb^{3+} centres maintains the first-order C_3 local symmetry. Moreover, the discrete structure observed in some of the selectively excited emission spectrum indicates a discrete ensemble of slightly different crystalline fields. At this

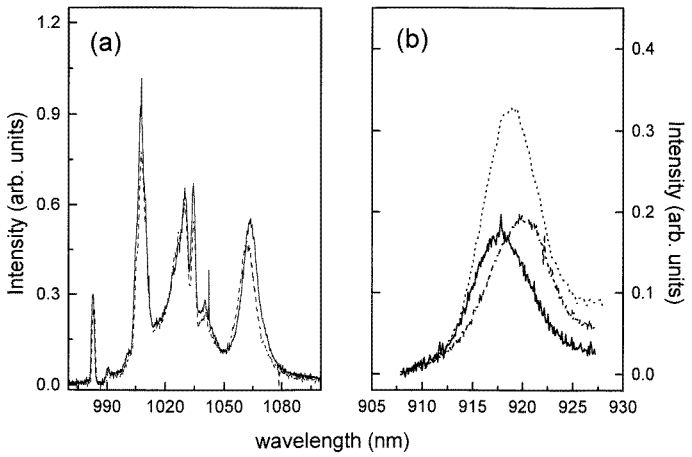

Figure 5. (a) Selectively excited emission spectra at low temperature for two different excitation wavelengths. Continuous line $\lambda_{exc} = 915$ nm; dashed line $\lambda_{exc} = 926$ nm. (b) Low temperature absorption and excitation spectra for a single inter-Stark transition $^2F_{7/2}(1) \rightarrow {}^2F_{5/2}(3)$. Dotted line: absorption spectrum; dashed and continuous line: excitation spectra for $\lambda_{em} = 1054.4$ nm and 1070.4 nm respectively.

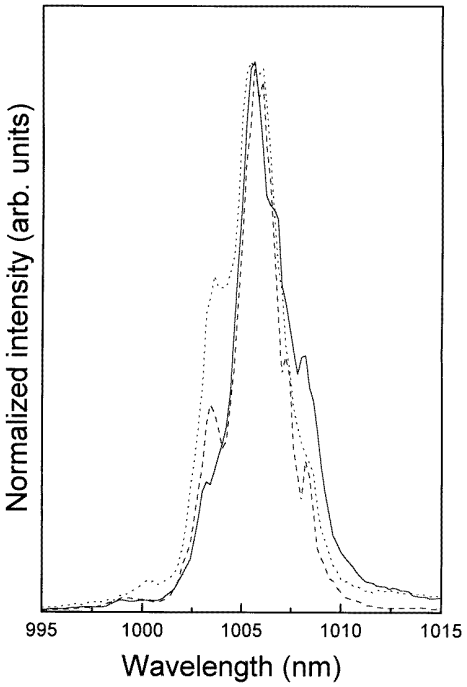

Figure 6. Low temperature selectively excited emission spectra for a single Stark transition $^2F_{5/2}(1) \rightarrow {}^2F_{7/2}(1)$. The spectra have been normalized in intensity. Continuous line $\lambda_{exc} = 980$ nm; dashed line $\lambda_{exc} = 980.95$ nm and dotted line $\lambda_{exc} = 981$ nm.

point, it is important to mention that the number of centres observed is at least four, similar to other RE^{3+} doped $LiNbO_3$. However, though the presence of Yb^{3+} multisites is clearly

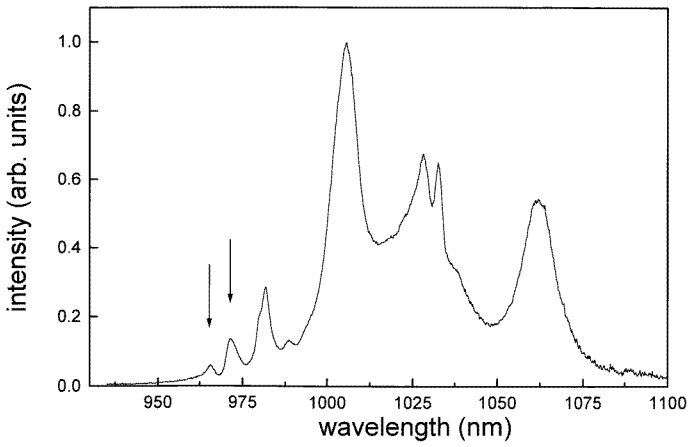

Figure 7. Yb^{3+}:Mg:$LiNbO_3$ low temperature emission spectra under excitation at 907 nm.

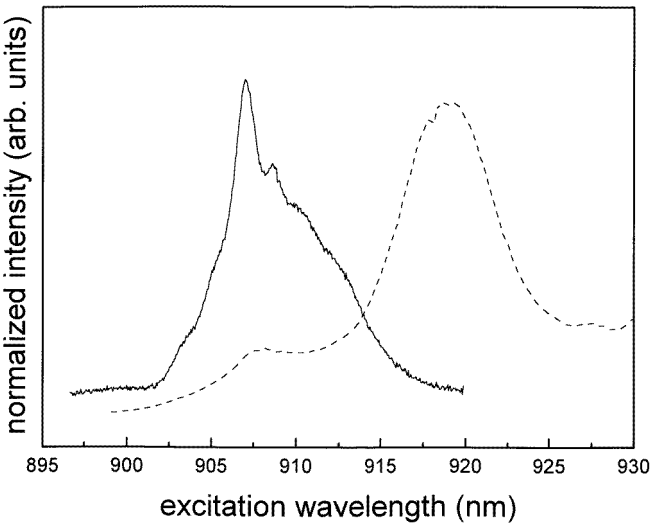

Figure 8. Low temperature excitation spectra of Yb^{3+}:Mg:$LiNbO_3$. Continuous line $\lambda_{em} = 972.5$ nm; dashed line $\lambda_{em} = 981$ nm.

demonstrated by this technique, the total isolation of a single-site emission line has not been possible due to the strong overlapping of the emission lines from the different centres, and, thus, the location of the crystal field components of each particular centre is not possible.

The presence of non-equivalent centres has also been reported for a variety of RE ion doped $LiNbO_3$ [17]. The structure of these centres has been explained as a result of the different displacements around the average position determined by RBS/channelling [10]. Although a full understanding of the structure of these centres is still lacking, it is believed that its origin lies in the mechanisms needed for local charge compensation and in the defects associated with the non-stoichiometry of the $LiNbO_3$.

Figure 3 showed how MgO codoping induced a new absorption band at 907 nm which could be associated with different Yb^{3+} centres than those corresponding to the singly doped

crystals. The existence of these new centres is also detected by the photoluminescence spectra under excitation at this new absorption band. As shown in figure 7, when exciting at 907 nm two new emission bands appear at 964 nm and 972 nm. Figure 8 shows two partial excitation spectra monitoring at two emission wavelengths: one associated with Yb^{3+} centres related to the presence of Mg ions in the crystals (972 nm) and one observed for Yb singly doped crystals (980 nm). These spectra unambiguously show an ensemble of Yb^{3+} ions with a quite different crystal field from those obtained for the singly doped crystals. As can be observed, the excitation spectrum of the 972 nm line shows a relatively complex band peaking at 907 nm, in agreement with the absorption spectra of the Mg–Yb co-doped crystal. The excitation corresponding to the 980 nm emission mainly consists of the line at 918 nm, observed in both singly and doubly doped crystals, though a small contribution of the band at 907 nm (associated with the presence of MgO) is also detected which seems to indicate a possible energy transfer from the different Yb centres, as shown for other systems [14].

4. Conclusion

The absorption and emission spectra of the Yb^{3+}:$LiNbO_3$ system can be well interpreted considering C_3 symmetry for Yb^{3+} ions. However, several Yb^{3+} centres with slightly different energy schemes contribute to the optical spectra. The different centres can be related to Yb^{3+} ions inside the Li^+ octahedron but with different slight deviations from the regular Li site, as occurs for other RE^{3+} ions when they enter $LiNbO_3$ crystals.

Acknowledgments

This work has been supported by the Comisión Interministerial de Ciencia y Tecnología (CICYT) under project No MAT-95-0152. EM gratefully acknowledges the Spanish Ministry of Educacion for an FPI fellowship. The authors wish to thank Professor J García Solé for a critical reading of the manuscript and J A Sanz García for the crystal growth.

References

[1] Córdova-Plaza A, Digonnet M and Shaw H J 1987 *IEEE J. Quantum Electron.* **13** 262
[2] Jones J K, de Sandro J P, Hempstead M, Sheperd D P, Large A C, Tropper A C and Wilkinson J S 1995 *Opt. Lett.* **20** 1477
[3] Kuleshov N V, Lagatsky A A, Shcherbitsky V G, Mikhailov V P, Heumann E, Jensen T, Diening A and Huber G 1997 *Appl. Phys.* B **64** 409
[4] Schaffers K I, De Loach L and Payne S 1996 *IEEE J. Quantum Electron.* **32** 741
[5] Long X, Tong Y P, French P M W and Taylor J R 1997 *Opt. Comm.* **141** 162
[6] Bruesselbach H and Sumida D A 1996 *Opt. Lett.* **21** 480
[7] Auzel F 1966 *C. R. Acad. Sci., Paris* **262** 1016
Ennen H, Pomrecke G, Grasso M and Bridenbaugh P M 1985 *J. Appl. Phys.* **57** 2182
[8] Burns G, O'Kane D F and Title R S 1968 *Phys. Rev.* **167** 314
[9] Polgár K, Kovács L, Földvári I and Cravero I 1986 *Solid State Commun.* **59** 375
[10] Lorenzo A, Loro H, Muñoz Santiuste J E, Terrile M C, Boulon G, Bausá L E and García Solé J 1997 *Opt. Mater.* **8** 55
[11] Ellens A, Andres H, Ter Heerdt M L H, Wegh R T, Meijerink A and Blasse G 1996 *J. Lumin.* **66/67** 240
[12] de Deloach L, Payne S A, Kway W L, Tassano J B, Dixit S N and Krupke W F 1994 *J. Lumin.* **62** 85
[13] Montoya E, Sanz-García J A and Bausá L E *Spectrochim. Acta* A at press
[14] García Solé J, Petit T, Jaffrezic H and Boulon G 1993 *Europhys. Lett.* **24** 719
[15] Weber M J 1971 *Phys. Rev.* B **4** 9
[16] de Bernabé A, Prieto C and de Andrés A 1996 *J. Appl. Phys.* **79** 143
[17] García Solé J 1994 *Phys. Scr.* T **55** 30